

**Development of a Method for Fast and Automatic Radiocarbon Measurement of Aerosol  
Samples by Online Coupling of an Elemental Analyzer with a MICADAS AMS**

Salazar, G. <sup>a</sup>; Zhang, Y. L. <sup>a,b</sup>; Agrios, K. <sup>a,b</sup>; Szidat, S. <sup>a</sup>

<sup>a</sup> *Department of Chemistry and Biochemistry & Oeschger Centre for Climate Change Research,  
University of Bern, 3012 Bern, Switzerland.*

<sup>b</sup> *Paul Scherrer Institut (PSI), 5232 Villigen, Switzerland.*

Corresponding Author

Salazar Gary, Ph.D.

Tel.: +41-31-6314263

Email: gary.salazar@dcb.unibe.ch

**Accepted version**

**Published in**

**Nuclear Instruments and Methods in Physics Research B 361 (2015) 163-167**

**<http://dx.doi.org/10.1016/j.nimb.2015.03.051>**

## **ABSTRACT**

A fast and automatic method for radiocarbon analysis of aerosol samples is presented. This type of analysis requires high number of sample measurements of low carbon masses, but accepts precisions lower than for carbon dating. The method is based on online Trapping CO<sub>2</sub> and coupling an elemental analyzer with a MICADAS AMS by means of a gas interface. It gives similar results to a previously validated reference method for the same set of samples. This method is fast and automatic and typically provides uncertainties of 1.5% to 5% for representative aerosol samples. It proves to be robust and reliable and allows for overnight and unattended measurements. A constant and cross contamination correction is included, which indicates a constant contamination of  $1.4 \pm 0.2 \mu\text{g C}$  with  $70 \pm 7 \text{ pMC}$  and a cross contamination of  $(0.2 \pm 0.1)\%$  from the previous sample. A real-time online coupling version of the method was also investigated. It shows promising results for standard materials with slightly higher uncertainties than the trapping online approach.

## 1. INTRODUCTION

For environmental and climate sciences, it is important to apportion the origin of the atmospheric aerosols between wood burning, biogenic emissions and fossil fuel combustion [1]. This can be achieved by analyzing radiocarbon in the aerosols using accelerator mass spectrometry (AMS). However, sample preparation is highly effort and time consuming (~1 hr/sample) [2, 3]. When analytical and separation methods are included in the sample preparation for radiocarbon measurement, the analysis of the compounds from each fraction not only makes the process even longer, but the recovered carbon mass is split and falls in the low microgram range. Some examples are compound-specific analysis of environmental pollutants and carbon cycle markers [4, 5] and analysis of radiolabelled markers for biomedical studies [6]. For all the cases explained above, it is possible to improve the throughput by coupling the separation/combustion technique with the AMS by taking advantage of a gas interface that specifically and efficiently delivers the CO<sub>2</sub> into the gas ion source of the AMS. This paper describes the validation of the method of a previous study [7] for the fast and automatic analysis of the total carbon (TC) from aerosol samples at the microgram level. In such method, an elemental analyzer (EA) is coupled with the AMS. Radiocarbon method development requires the quantification of the constant and cross contamination (also known as memory effect) in order to make corrections to the drifted radiocarbon measurements [8-10]. Therefore, we apply a mathematical model that handles constant contamination. As a difference with previous works, this drift model also includes cross contamination. For validation, the Trapping online coupling was compared with a reference method for aerosol samples. Finally, this paper briefly shows the proof-of-principle of a new gas interface that allows online coupling the EA with AMS. Potentially, these online methods may be applied to couple other separation techniques with AMS like liquid or gas chromatography.

## 2. MATERIALS AND METHODS

The schematic of the Trapping online coupling is shown in Figure 1 and the detailed method can be found elsewhere [7, 8]. Solid samples or standards are tightly packed in tin foil for flash combustion. They are loaded into the oxidation oven of the EA at 850 °C by an autosampler and combusted with a pulse of oxygen. The EA directs the gases through a water trap containing Sicapent (Merck, Germany) and through a zeolite trap which is later heated up stepwise by the EA to release N<sub>2</sub>, CO<sub>2</sub> and residual gases at different temperatures. The outlet of the EA is connected to a gas interface system (GIS) through a 1/16'' O.D. tubing (10 m long). The flow is directed to a second zeolite trap (zeolite X13, Sigma-Aldrich, Germany) located at the GIS at 80 mL/min. The details of the trap can be found elsewhere [7, 8]. Consecutively, the GIS trap is heated up to 450 °C, the CO<sub>2</sub> expands into a syringe of known volume, the carbon amount is measured manometrically, helium is added to make a mixture of 10% CO<sub>2</sub> at ~0.16 MPa, and finally the mix is transferred into the gas ion source of a MICADAS AMS at ~40 µL/min. At the same time that the sample is being measured, a flushing step is carried out to the EA-GIS system during 4 min. It consists on running a blank combustion in the EA at 100 mL/min, including heating up the CO<sub>2</sub> trap of the EA. This high flow is directed to the GIS trap which at the same time is being heated up for flushing. The whole procedure is automatic and controlled by a LabView program based on an earlier version described by Wacker et al. [11].

The standards were solid crystals of sodium acetate (fossil; p.a., Merck, Germany), C5, C6 and C7 from IAEA and oxalic acid II from NIST (SRM 4990C) with <sup>14</sup>C/<sup>12</sup>C ratios of 23.05±0.02 pMC, 150.61±0.11, 49.35±0.12 pMC and 134.07±0.05 pMC, respectively. The next experiment consists on punching out 4 to 10 pieces (dia. 4 mm) from real aerosol filters and wrapping them in tin foil (5 pieces/foil). The same filters were analyzed with a reference method for validation purposes. This reference method includes burning the samples with an OC/EC analyzer, trapping

the CO<sub>2</sub> in quartz ampoules and analyzing the CO<sub>2</sub> with the GIS interface. The experimental details can be found elsewhere [2].

The online coupling of the EA with the AMS was done by separating the high load of the gas carrier (helium) from the microgram-level CO<sub>2</sub> using two flow separators. A flow separator (FS) is gas interface for online coupling, developed in our laboratory. The description and fundamentals of a FS can be found in a separated publication [12].

### 3. RESULTS AND DISCUSSION

#### 3.1 Mathematical basis of the contamination drift model for the Trapping online coupling

Our assumptions are based on previous works [8-10]. The first hypothesis of the model (equation 1) is that each time a sample of carbon mass ( $m_s$ ) and <sup>14</sup>C/<sup>12</sup>C ratio ( $R_s$ ) is injected in the EA-GIS system, it is mixed with a contaminant that is constant with respect to its mass and isotopic ratio ( $m_k$  and  $R_k$ ). Equation 1 indicates how much the measured ratio of the sample ( $R_m$ ) drifts from the real ratio of the sample  $R_s$ . It is assumed that the contamination is mostly due to the tin foil.

$$R_m = \frac{m_s R_s + m_k R_k}{m_s + m_k} \quad \text{Eq.1}$$

Equation 1 can be written as the drift of the measured ratio ( $drift = R_m - R_s$ ) by subtracting  $R_s$  from both sides (equation 1b).

$$drift = \frac{m_s R_s + m_k R_k - (m_s + m_k) R_s}{m_s + m_k} \quad \text{Eq. 1b}$$

After term cancellations, the approximation that the mass of the contaminant is much smaller than the sample mass ( $m_s + m_k \sim m_s$ ) is applied and equation 1 can be rewritten as

$$drift = \frac{m_k}{m_s} (R_k - R_s) \quad \text{Eq. 2}$$

The cross contamination (or memory effect) is the fraction ( $\phi$ ) of carbon of the previous sample ( $m_x$ ) that remains inside the EA-GIS system after unloading and cleaning the system. After including this concept, equation 2 can be rewritten as

$$drift = \frac{m_k}{m_s} (R_k - R_s) + \frac{\phi m_x}{m_s} (R_x - R_s) \quad \text{Eq. 3}$$

Equation 3 shows that the drift is inversely proportional to the sample mass. However, the drift is higher for high amounts of the contaminant. Also the sign and magnitude of the drift depends on the difference between the ratios of the sample and the contaminant. The cross contamination presents a similar effect over the drift. We think that the drift model makes sense because the model covers these expected relationships. After finding the contamination parameters that characterize our system, it is possible to correct any measured value by subtracting the contamination as it is shown in the mass conservation principle of equation 4.

$$R_m^{corr} = \frac{m_s R_m - m_k R_k - \phi m_x R_x}{m_s - m_k - \phi m_x} \quad \text{Eq. 4}$$

The corrected  $R_m$  can also be obtained by subtracting the calculated drift (equation 3) from the measured value.

$$R_m^{corr} = R_m - drift \quad \text{Eq. 5}$$

The reason of the minus in equation 5 is to make the direction of the  $R_m$  correction to be opposite to the direction of the drift. For example, a negative drift will make the corrected  $R_m$  to be higher than the measured ratio ( $R_m$ ). The uncertainty of the corrected  $R_m$  can be calculated by error propagation of equation 5 (equation 6).

$$u_m^{corr} = \sqrt{u_m^2 + u_{drift}^2} \quad \text{Eq. 6}$$

In equation 6,  $u_m$  is the measurement uncertainty of  $R_m$  and  $u_{drift}$  is the confidence band of the drift model. All the uncertainties are calculated for a probability of 68% ( $1\sigma$  range).

### 3.2 Constant contamination of the Trapping online coupling

Figure 2 shows how the data for the 3 different standard materials fit into the model, and the fit presents a good coefficient of determination. Basically, the model is the non-linear least-squares regression (nlr) of equation 2. The nlr and the confidence bands are weighted with the inverse of the relative uncertainty of  $R_m$ , i.e.  $(u_m/R_m)^{-1}$ . The constant contaminant parameters ( $R_k$  and  $m_k$ ) extracted from the fit are  $70\pm 3$  pMC and  $1.4\pm 0.1$   $\mu\text{g C}$ , which indicates that probably the contamination is a mixture of modern and fossil carbon dispersed in the laboratory air and in the tin foil. Similar  $R_k$  values were observed earlier by Ruff et al [7]. Because the corrected  $R_m$  is calculated from the subtraction of the drift from the measured  $R_m$  value, consequently the uncertainty of this correction can be determined by the error propagation of these two variables (See equations 5 and 6). The uncertainty of the drift ( $u_{drift}$ ) is equal to the confidence interval of the drift model. The uncertainty of the measured  $R_m$  comes from the counting statistics of the individual data. This applies for the whole paper. The high  $u_m$  values and the measurement dispersion at low masses explain the increase of the uncertainty of the corrected  $R_m$  at low masses. For example, the 3 standard materials at 10  $\mu\text{g C}$  show approximately the same uncertainty (6 pMC), which means 100%, 12% and 4.8% for fossil, C7 and oxalic acid II, respectively. On the other hand, at 50  $\mu\text{g C}$ , the corrected  $R_m$  uncertainties are 50%, 3% and 1.5% for the same standards. In the other hand, the reference method typically gives uncertainties of 1% for higher than 50  $\mu\text{g C}$  and 4% for around 10  $\mu\text{g C}$ .

Figure 2 indicates that the drift from the nominal value is minimum at large sample masses. At low masses, the drift increases faster for the fossil and oxalic acid II than for the C7; because the difference of the  $^{14}\text{C}/^{12}\text{C}$  concentration between C7 and the contaminant is smaller than the difference for the other standards. The similar behavior of the drifts for the red and blue groups shows that the constant contamination does not change considerably over a 3-months period which indicates that it is reliable to use the same parameters over long periods of time. The averages of the corrected  $R_m$  values for the oxalic acid II, C7 and fossil data sets are  $134\pm 2$ ,  $49\pm 1$  and  $-0.5\pm 0.8$ , respectively. Grubb's tests was used to identify outliers within each data set of the corrected  $R_m$  values using a probability of 95%; and it was found 1 outlier in the fossil data set from a total of 77 values. After withdrawing the outlier, one-sample  $t$ -tests show no significant difference between the average of the corrected  $R_m$  with its respective nominal value. In short, the corrected  $R_m$  values are well distributed around their respective nominal values.

### 3.3 Constant contamination in combination with cross contamination for the Trapping online coupling

For adding and controlling the cross contamination, injections of oxalic acid II are intercalated with fossil material as explained in the experimental. The cross contamination factor  $\phi$  obtained from the fit in Figure 3 is  $(0.2\pm 0.1)\%$ , which means that 0.2% of the carbon of the previous sample mixes and cross contaminates the next injection. In contrast, Ruff et al [8] measured  $\phi = 0.5\%$  using a very similar system as ours. We suppose that the difference is due to our flushing step, which cleans better the  $\text{CO}_2$  traps of the EA-GIS system (see experimental section). The  $R_k$  and  $m_k$  for this constant-cross contamination fit are  $70\pm 7$  pMC and  $1.4\pm 0.2$   $\mu\text{g C}$ . The shape of the model, confidence bands and corrections are similar to the results for constant contamination (Fig. 2); however, the  $^{14}\text{C}/^{12}\text{C}$  ratios are higher, indicating the extra contribution of the cross contamination in the overall drift. The average value of the corrected  $R_m$  for the fossil data set is



$0.04 \pm 0.7$  and it was found 1 outlier out of 23 values (same test as in the constant contamination section). Moreover, the data set passed the one-sample  $t$ -test with the nominal value. Therefore, the corrected  $R_m$  values are close to the nominal value.

The uncertainty of the corrected  $R_m$  is calculated with the error propagation of equation 5, but it is also possible to use the error propagation of equation 4. This was not done, because the uncertainty of  $m_s$  can hardly be evaluated for the experimental range of masses. If the drift model is applied separately to the data groups related to the blue and red closed circles in Figures 2 and 3, the respective parameters show no significant difference taking in account their uncertainty ranges (data not shown). Nevertheless, the uncertainties of  $R_k$  show significant difference when calculated for the different data groups. The uncertainties of  $R_k$  measured for the blue and red data groups in Figure 3 ( $u_k = 8$  and 19 pMC, respectively) are higher than the uncertainties of  $R_k$  measured with the whole data set ( $u_k = 7$  pMC), which indicates that the number of measurements determine the quality of the determinations of  $R_k$  and  $m_k$  in our model.

Independently of the drift model experiments, a direct measurement of  $R_k$  and  $m_k$  was carried out. Assuming that the blank from the tin foil for encasing the samples is the main cause of the constant contamination. 10 to 15 foils were tightly compacted without adding any other source of carbon and they were analyzed with the Trapping online system for 4 repetitions. The average values for  $R_k$  and  $m_k$  were  $59 \pm 13$  pMC and  $1.0 \pm 0.1$   $\mu\text{g C/foil}$ . The results are similar to the values obtained with the drift model ( $70 \pm 7$  pMC and  $1.4 \pm 0.2$   $\mu\text{g C}$ ).

### 3.4 Comparison of the Trapping online coupling with a reference method for aerosol samples

Figure 4 shows the measured  $^{14}\text{C}/^{12}\text{C}$  ratios for TC from real aerosol samples measured with a reference method [2] and with the Trapping online method. The constant and cross contamination correction is applied to the data. The contamination correction does not change considerably the

measured  $^{14}\text{C}/^{12}\text{C}$  ratios, because all carbon masses of the samples are large (30  $\mu\text{g}$  to 80  $\mu\text{g}$ ). The fitting of the data of figure 4 present a slope of  $1.021 \pm 0.007$ , there is no intercept and it has a very strong correlation. Therefore, both methods provide similar results for the range of measured ratios. However, from the point of view of the turn-around time, 4 samples can be analyzed in one hour with the Trapping online method, while the measurement of only one sample is possible with the reference method. Furthermore, the Trapping online method allows to run the gas measurements overnight and without human supervision. In summary, the data from Figures 2, 3 and 4 clearly shows that the Trapping online method is robust and reliable.

In Figure 4, the uncertainties for the Trapping online method range from 1.5% to 5% while for the reference method, they ranges from 1% to 2%. The Trapping online method has larger uncertainty than the reference method. Nevertheless, this is acceptable for aerosol research, as other uncertainty components typically dominate the final uncertainty, such as blank correction of the filters used for collection of the aerosols, the reference value for the conversion of  $^{14}\text{C}$  measurement results into the non-fossil fraction of the sources, and the uncertainty of the concentration measurements of TC or its sub-fractions [13].

### 3.6 Real-time coupling of EA with AMS

We used a flow separator (FS) as a gas interface for online coupling the EA with the AMS (Figure 5). A complete description of the FS can be found in this publication [12]. Basically, the FS separates most of the helium carrier (70 mL/min down to 1 mL/min) taking advantage of its low axial momentum which is due to its low molecular weight relative to  $\text{CO}_2$ . In that way, it is possible to keep the high vacuum and ionization efficiency of the ion source of the AMS with acceptable losses of  $\text{CO}_2$ . The data for a peer-review paper about the characteristics of the FS interface are still under preparation. The fact that we can state about the FS, in the present paper

is that it allows us to take radiocarbon measurements as described in the experimental section and the vacuum of the ion source stays around  $5 \times 10^{-6}$  mbar. Typically, the  $^{12}\text{C}^+$  current and the  $^{14}\text{C}$  count rate present peaks of similar width as the peak measured by the EA, which demonstrates that this coupling is truly a real-time online method. This also indicates the potential application of the FS for coupling other separating analytical techniques with AMS instruments. Table 1 presents the  $^{14}\text{C}/^{12}\text{C}$  ratio of different standard materials without contamination corrections. The  $^{14}\text{C}/^{12}\text{C}$  ratio was averaged over the range where the  $^{13}\text{C}/^{12}\text{C}$  ratio is relatively stable, which is close to the full width at half maximum of the  $^{12}\text{C}^+$  current peak. The uncertainties for the Real-time online coupling range from 1.6 to 4 pMC depending on the measured  $^{14}\text{C}/^{12}\text{C}$  ratio, which corresponds to 2.6%, 5% and 7% for C6, C7 and C5, respectively. In contrast, the typical uncertainties for the Trapping online method range from 1.5% to 5% for the same range of  $^{14}\text{C}/^{12}\text{C}$  ratios and carbon masses. The reason of the higher uncertainties for the Real-time online method is the shorter measurement time that leads to lower number of  $^{14}\text{C}$  counts (see Figure 5 and Table 1). In spite of the high uncertainties, the nominal and measured values are within the 1- $\sigma$  range. We consider that the online EA-AMS method is useful for fast screening and when precision can be sacrificed for gaining speed (10 min/sample). Further investigation is necessary to optimize this hyphenation technique.

#### **4. CONCLUSIONS**

The Trapping online method gives similar results to a previously validated reference method for the same set of samples having a broad range of  $^{14}\text{C}/^{12}\text{C}$  concentrations. It is fast and automatic (15 min/sample and overnight unattended mode) compared with the reference method (1 hr/sample).

The validated Trapping online method proves to be fast, robust and reliable for aerosol samples. The Real-time online method looks promising for even faster analysis or for tracing or surveying the  $^{14}\text{C}$  of the sample. Its results are similar to the nominal values of the standard materials, but the uncertainties are slightly larger than for the Trapping method. With different degrees of precision, both methods are useful depending on how much the user can sacrifice precision for gaining speed.

The constant and cross contamination model explains and corrects the drift of the radiocarbon measurements of the Trapping online method for aerosol samples. The data shows that the mass and  $^{14}\text{C}/^{12}\text{C}$  ratio of the constant contamination are  $1.4\pm 0.2 \mu\text{g C}$  and  $70\pm 7 \text{ pMC}$ . The cross contamination is  $0.2\pm 0.1 \%$  of the previous sample. The model is reliable and robust because the data fitted well and there are not considerable changes of the parameters over time (3 months). However, the uncertainty rapidly increases at low masses (e.g. 4.8% for oxalic acid II at  $10 \mu\text{g C}$ ) compared to high masses (e.g. 1.5% for the same standard at  $50 \mu\text{g C}$ ).

#### **5. ACKNOWLEDMENT**

We thank our laboratory technicians Michael Battaglia and Edith Vogel for their support with the instrumentation.

## 6. REFERENCES

- [1] S. Szidat, T. M. Jenk, H.-A. Synal, M. Kalberer, L. Wacker, I. Hajdas, A. Kasper-Giebl, and U. Baltensperger *J. Geophys. Res.*, 111 (2006) D07206.
- [2] Y. L. Zhang, N. Perron, V. G. Ciobanu, P. Zotter, M. C., Minguillón, L. Wacker, A.S.H. Prévôt, U. Baltensperger and S. Szidat *Atmos. Chem. Phys.*, 12 (2012) 10841-10856.
- [3] S.M. Fahrni et al., *Nucl. Instr. and Meth. Phys. Res. B*, 268 (2010) 787-789.
- [4] L.A. Currie, T.I. Eglinton, A. Benner Jr., A. Pearson, *Nucl. Instr. and Meth. Phys. Res. B* 123 (1997) 475–486.
- [5] J. M. Ahad, R. S. Ganeshram, C. L. Bryant, L. M. Cisneros-Dozal, P. L. Ascough, A. E. Fallick, G. F. Slater, *Marine Chemistry* 126 (2011) 239-249.
- [6] A. Thomas, T. Ognibene, P. Daley. *Anal. Chem.* (2011) 9413-9417.
- [7] M. Ruff, S. Szidat, H. W. Gaggelera, M. Suter, H. Synal, L. Wacker. *Nucl. Instr. and Meth. Phys. Res. B*, 268 (2010) 790-794.
- [8] M. Ruff, S. Fahrni, H. W. Gaggeler, I. Hajdas, M. Suter, H.-A. Synal, S. Szidat, L. Wacker, *Radiocarbon*, 52 (2010) 1645–1656.
- [9] G.M. Santos, J.R. Southon, S. Griffin, S.R. Beaupre, E.R.M. Druffel, *Nucl. Instr. and Meth. Phys. Res. B* 259 (2007) 293–302.
- [10] C.R. Bronk, R.E.M. Hedges, *Nucl. Instr. and Meth. Phys. Res. B*, 52 (1990) 322–326.
- [11] L. Wacker, S.M. Fahrni, I. Hajdas, M. Molnar, H.-A. Synal, S. Szidat, Y.L. Zhang, *Nucl. Instr. and Meth. Phys. Res. B*, 294 (2013) 315–319.

[12] G. Salazar, S. Szidat. *Flow dynamics technique for sampling and separation of neutrals from analytes based on their axial momentum density differences*. Poster presented at the annual meeting of the American Society for Mass Spectrometry (2014) Baltimore, U.S.A.

[13] P. Zotter, I. El-Haddad, Y. Zhang, P.L. Hayes, X. Zhang, Y.H. Lin, L. Wacker, J. Schnelle-Kreis, G. Abbaszade, R. Zimmermann et al. *J. Geophys. Res. Atmos.*, 119 (2014) 6818–6835.

## 7. TABLES

Table I.  $^{14}\text{C}/^{12}\text{C}$  analysis of IAEA standards (n=2) using the Real-time online method with uncertainty at 1- $\sigma$  range. The total number of  $^{14}\text{C}$  counts ranged from 280 to 2500 for the different standards using sample masses of  $\sim 50 \mu\text{g C}$ .

Standard	$^{14}\text{C}/^{12}\text{C}$ (pMC)	Nominal value (pMC)
C5	$24.6 \pm 1.6$	23.05
C7	$50.3 \pm 2.5$	49.53
C6	$155 \pm 4$	150.61

## 8. FIGURE CAPTIONS

Figure 1. Schematic of the elemental analyzer online coupling with AMS using a gas interface system GIS (Trapping online method). TCD means thermal conductivity detector.

Figure 2. Constant contamination model for 3 different standard materials. The closed blue and red circles show the measured  $^{14}\text{C}/^{12}\text{C}$  ratios for two different measurement dates with a time lag of 3 months; the blue closed circles were taken in an overnight unattended measurement. The red line represents the drift model ( $r^2 = 0.84$ ) with confidence bands (uncertainty of the model) for a probability of 68% ( $1\sigma$ ). Black opened squares show corrected  $R_m$  ratio calculated with equation 4 with confidence bands and the nominal value.

Figure 3. Cross contamination (memory effect) model. The previous sample mass ( $m_x$ ) is almost constant for all data points ( $\sim 50 \mu\text{g}$ ). The closed circles show in blue and red measured  $^{14}\text{C}/^{12}\text{C}$  ratios for two different measurement dates with a time lag of 3 months; the blue closed circles were taken in an overnight unattended measurement. The red line represents the drift model ( $r^2 = 0.94$ ) with confidence bands for a probability of 68% ( $1\sigma$ ). Black opened squares show corrected  $R_m$  ratio calculated with equation 4 with confidence bands calculated with equation 6 and the nominal value.

Figure 4. Comparison of the Trapping online method with the reference method for TC from aerosol samples with  $1\sigma$  uncertainties. Blue and red symbols indicate for two different measurement dates with a time lag of 3 months, whereof the blue closed circles were taken in an overnight unattended measurement. The red closed circles group was taken in a semi-attended fashion and the measurement dates of both groups were 3 months apart.



Figure 5. Schematic of the Real-time online coupling using two flow separators. Typical results are also included. a) Schematic b) EA (Thermal Conductivity Detector) and AMS ( $^{12}\text{C}^+$  current) signals vs time. c)  $^{14}\text{C}$  count rate vs time. The  $^{14}\text{C}/^{12}\text{C}$  is averaged over the time interval indicated by the double headed arrow.

## 9. FIGURES

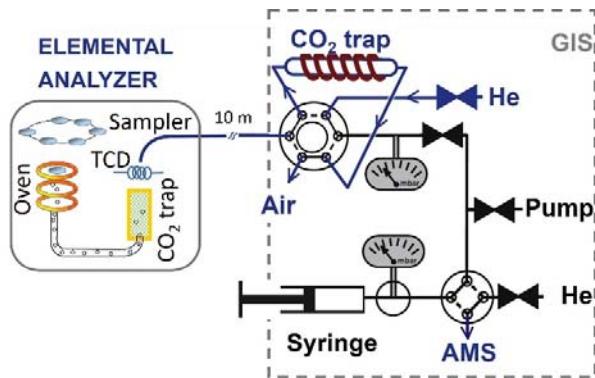


Figure 1

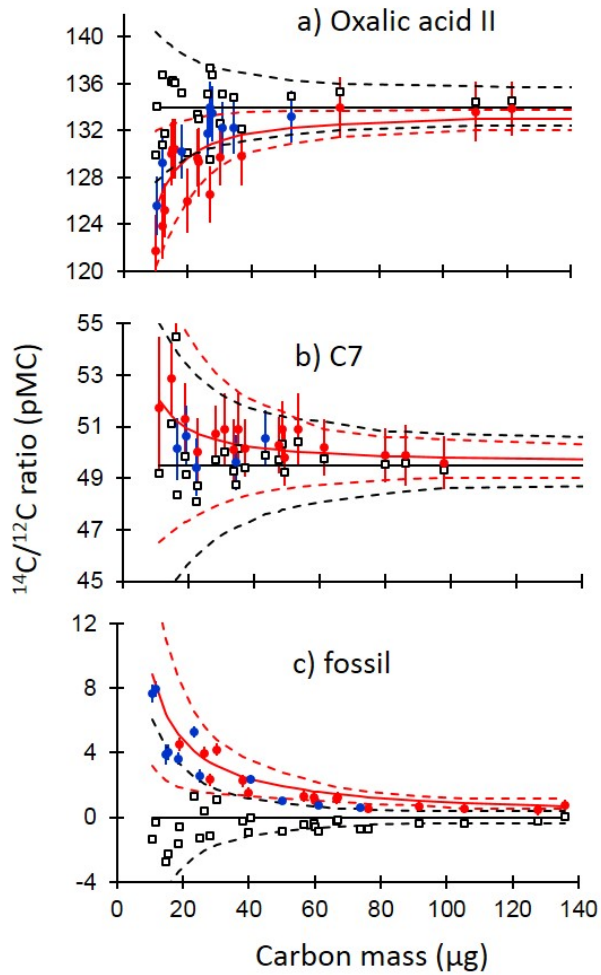


Figure 2

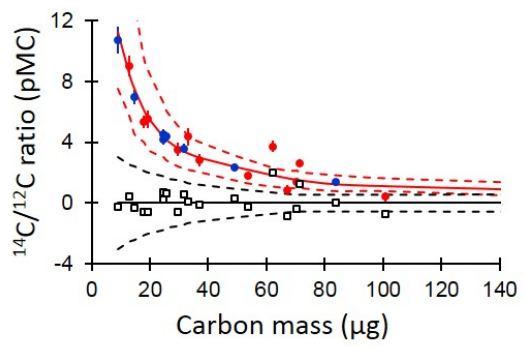


Figure 3

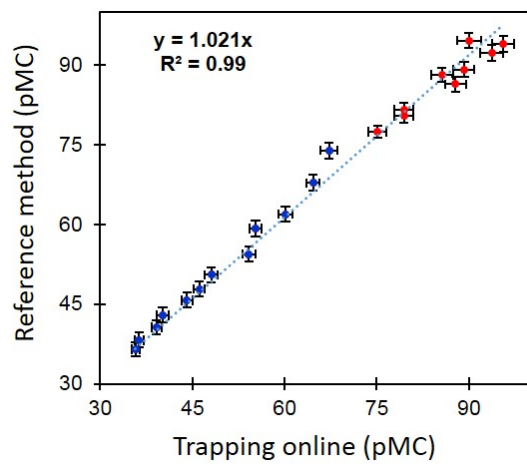


Figure 4

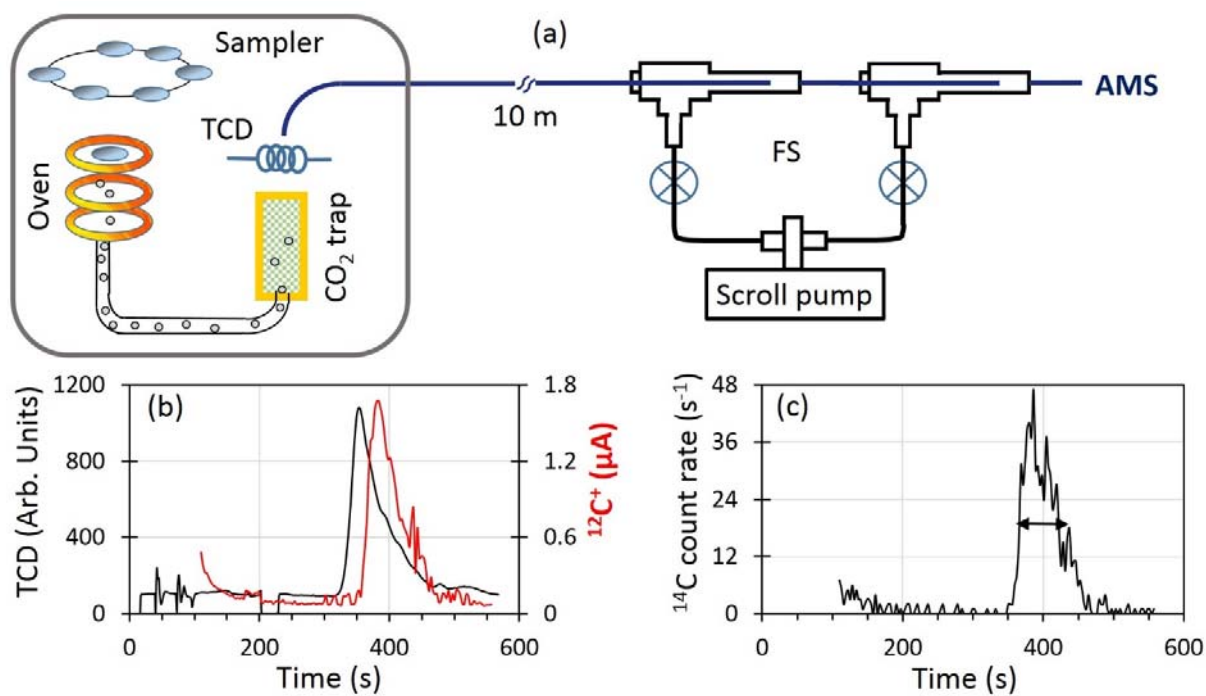


Figure 5